ACADEMIC PRESS

Available online at www.sciencedirect.com

SCIENCE DIRECT®

Journal of Sound and Vibration 263 (2003) 853–870

JOURNAL OF SOUND AND VIBRATION

www.elsevier.com/locate/jsvi

Statistical damage identification of structures with frequency changes

Yong Xia, Hong Hao*

School of Civil and Structural Engineering, Nanyang Technological University, Nanyang Avenue, 639798 Nanying, Singapore

Received 1 December 2000; accepted 15 July 2002

Abstract

Model updating methods based on structural vibration data have being rapidly developed and applied to detect structural damage in civil engineering. But uncertainties existing in the structural model and measured vibration data might lead to unreliable damage detection. In this paper a statistical damage identification algorithm based on frequency changes is developed to account for the effects of random noise in both the vibration data and finite element model. The structural stiffness parameters in the intact state and damaged state are, respectively, derived with a two-stage model updating process. The statistics of the parameters are estimated by the perturbation method and verified by Monte Carlo technique. The probability of damage existence is then estimated based on the probability density functions of the parameters in the two states. A higher probability statistically implies a more likelihood of damage occurrence. The presented technique is applied to detect damages in a numerical cantilever beam and a laboratory tested steel cantilever plate. The effects of using different number of modal frequencies, noise level and damage level on damage identification results are also discussed.

1. Introduction

Many structures in their service life are inevitably subjected to deterioration and damage due to many factors such as environmental erosion, operating loads, fatigue, accidental bumping, etc. Because the structural failure could be catastrophic not only in terms of the loss in economy and life, but also in terms of the subsequent social and psychological impacts, structural damage detection is becoming a worldwide research subject. Current non-destructive test methods are

*Corresponding author. Current address: School of Civil and Resource Engineering, The University of Western Australia, Crawley, WA 6009, Australia.

E-mail address: hao@civil.uwa.edu.au (H. Hao).

0022-460X/03/$ - see front matter
PII: S0022-460X(02)01077-5

either visual or local experimental methods such as ultrasonic methods, electromagnetic methods, radiological methods, optical methods and thermal field methods. These methods are time consuming and costly, moreover, the location of the damage must be known a priori and the inspection area must be accessible.

A vibration-based method that examines the changes of vibration characteristics (such as natural frequencies, mode shapes and damping) of structures has been developed to detect the structural damage. This method is based on the fact that local damages usually cause decrease in the structural stiffness, which produces changes in the global vibration characteristics of the structure. When the changes of the vibration data are examined, the damage locations and magnitudes can be identified. The advantage of this method is that it is not necessary to know the damage locations beforehand. With the development of measurement equipment and signal processing techniques, the vibration properties of a structure can be measured more accurately and conveniently so that this method is rapidly developed and applied in civil, mechanical and aerospace engineering in the last decades.

The vibration data used to detect the structural damage include frequency response functions, natural frequencies, mode shapes, mode shape curvatures, modal flexibility, modal strain energy, etc. An extensive review can be found in Ref. [1]. Among these data types, natural frequency is used widely because it can be measured most conveniently and accurately. Moreover, natural frequencies are the global properties of the structure and thus they can be measured at a few locations or even at one point. Initial studies to detect damage with frequency changes mainly focus on forward method in which the measured frequencies are compared directly with the predicted data [2–4]. This forward technique can only give damage location and only be practical for a single damage scenario. Recently an inverse approach, namely model updating method is applied to identify damage, in which the parameters in a finite element (FE) model are adjusted so that the model predictions match the measured data in an optimal way [5–7]. It includes two-stage model updating processes: model improvement (or model tuning) and damage identification. In the first-stage model updating, using the measured vibration data at the undamaged state of a structure, the initial analytical FE model, namely IM, is tuned to obtain an updated model in the undamaged state denoted as UM. Then the UM is updated to obtain a model in the damaged state (DM) with the measured vibration data at the damaged state of the structure. The damage is identified by comparing the differences between UM and DM (usually the reduction of the stiffness parameters).

The efficiency of this damage identification algorithm relies on accuracy of the analytical FE model and the measured frequencies. Most studies assume that the analytical FE model is precise enough to represent the vibration properties of the structure and the measurements are accurate as well. In practice, however, there are many uncertainties during model updating procedure such as the FE modelling error and measurement noise [8]. Uncertainties in the FE model exist due to inaccurate physical parameters, non-ideal boundary conditions and structural non-linear properties. These are more true in civil engineering especially for concrete structures. On the other hand, measurement noise is inevitable. If the uncertainty level is larger than or close to the frequency changes due to damages, the true information is submerged in the noise thus the actual damaged members cannot be identified accurately and/or the healthy members may be wrongly detected as damaged. Therefore, it is very important to analyze the influences from both the FE modelling error and measurement noise on the damage identification results.

Some studies have considered the uncertainty effect on the model updating. Collins et al. [9] first derived a statistical identification procedure by treating the initial structural parameters as normally distributed random variables with zero means and specified covariance. Liu [10] considered the measurement noise effect on the damage detection with the perturbation method and Monte Carlo simulation algorithm. Papadopoulos and Garcia [11] presented a probabilistic damage detection methodology by considering the measurement noises. However, these studies only considered either FE modelling error or the measured data noise, and performed only the second-stage model updating.

To derive a robust statistical damage identification method with frequency changes that includes the uncertainties in both FE model and measured data simultaneously, a two-stage model updating algorithm with statistical approach is developed in this paper (Fig. 1). The first-stage updating is to derive the statistical FE model of the structure at the undamaged state, UM, by considering the statistical uncertainties of the initial analytical FE model (IM) and the noises in the measured frequencies of the undamaged structure as normally distributed random variables. The mean values and standard deviations of the stiffness parameters of UM are derived by using perturbation method. The second stage is to update the UM to derive a statistical FE model in the damaged state (DM) based on the measured frequencies in the damaged structure. The random noise in the measured frequencies corresponding to the damaged structure is also assumed as normally distributed. The statistics of the stiffness parameters of DM are similarly derived. The variations of the stiffness parameters in UM and DM are proved also having normal distributions by Monte Carlo simulation and goodness-of-fit test. Probability of damage existence (PDE) can be estimated by comparing the probability distributions of stiffness parameters of UM and DM. A higher PDE of a structural member implies a higher likelihood of the existence of damage in the member.

If the measurements of the undamaged structure are not available, which is true for most practical cases unless for newly constructed structures or laboratory test, the usual assumption

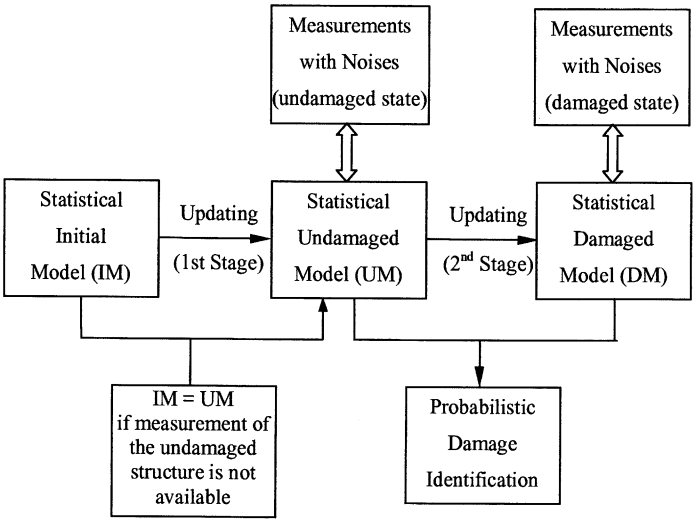

Fig. 1. Procedure of damage identification.

that the analytical model is precise has to be adopted. In such cases, the numerical frequencies are used as the baseline for model updating as used by many researchers [12]. But in the present study, the uncertainties in the FE model are included to directly obtain the statistical variations of stiffness parameters in UM without model updating. This, however, is a special case of the two-stage model updating developed in this paper and only the second-stage statistical model updating is applied.

A steel cantilever beam and a laboratory tested steel cantilever plate by other researchers [13] are used to illustrate the developed procedure. Some parametric calculations are performed to investigate the effects of using different number of modal frequencies, noise level as well as damage severity on the identification results.

It should be noted that in the present study only random noises, i.e., random errors in material properties and measured vibration signals are considered. Systematic errors such as those induced in FE model due to discretization and configuration error, and those in the measured signals owing to the environmental impacts and/or measurement set-up and equipment error, are not considered. Theoretically, it is possible to include the systematic errors in the following derivations by using non-zero mean values for the random variables. However, it will be difficult to determine the systematic error or non-zero mean values in practice. For example, the systematic changes owing to environmental impact such as temperature variation can only be determined by long-term monitoring of the structures. The systematic errors in the measured data can be avoided by careful calibrations of the equipment and measurement setting up. On the other hand, the systematic errors in the FE model induced by FE discretization, cannot be corrected by model updating. Usually, model updating is used to update material parameters and boundary conditions, not the FE mash. The normal way to reduce the FE discretization and configuration errors is to carry out convergence and patch tests of the FE mesh. Nevertheless, such systematic errors will certainly affect damage identification results. More studies by combining the FE modelling, model updating, long-term monitoring, measurement and signal processing techniques, are necessary to include both the systematic and random errors in the structural damage identification analysis.

2. Model updating with frequency changes

The free vibration of an undamped structure with N degrees of freedom is described by the eigenvalue problem as

$$(-\lambda_i[M] + [K])\{\phi_i\} = \{0\}, \quad i = 1, 2, \ldots, N, \tag{1}$$

where $[M]$ is the $N \times N$ symmetric mass matrix, $[K]$ is the $N \times N$ symmetric stiffness matrix, λ_i and $\{\phi_i\}$ are the ith eigenvalue and mass-normalized mode shape, respectively. When there are changes in the structural parameters, the vibration properties will change accordingly and eigenvalue problem can be similarly written as

$$(-\tilde{\lambda}_i[\tilde{M}] + [\tilde{K}])\{\tilde{\phi}_i\} = \{0\}, \quad i = 1, 2, \ldots, N, \tag{2}$$

where the tilde indicates the structural parameters and vibration properties in the changed state. From the above two equations, the changed structural parameters can be solved with the initial structural parameters and the measured eigenvalues in the changed state.

Assuming that the mass remains unchanged, the quantities in Eqs. (1) and (2) have

$$[\tilde{K}] = [K] + [\Delta K], \tag{3}$$

$$[\tilde{M}] = [M], \tag{4}$$

$$\tilde{\lambda}_i = \lambda_i + \Delta\lambda_i, \tag{5}$$

$$\{\tilde{\phi}_i\} = \{\phi_i\} + \{\Delta\phi_i\}. \tag{6}$$

Substituting Eqs. (3)–(6) into Eq. (2) and left-multiplying $\{\phi_i\}^{\mathrm{T}}$, the following can be derived by neglecting the high order terms:

$$\{\phi_i\}^{\mathrm{T}}[\Delta K]\{\phi_i\} = \Delta\lambda_i = \tilde{\lambda}_i - \lambda_i, \tag{7}$$

where $\{\ \}^{\mathrm{T}}$ represents the transposed vector. As usual, $[K]$ and $[M]$ are obtained by assembling the contribution of all m elements in the discrete FE model [6]. In particular,

$$[K] = \sum_{i=1}^{m}[K]_i = \sum_{i=1}^{m}\alpha_i[K^e]_i, \tag{8}$$

$$[M] = \sum_{i=1}^{m}[M]_i = \sum_{i=1}^{m}\beta_i[M^e]_i, \tag{9}$$

where $[K]_i$ and $[M]_i$ are, respectively, the ith elemental stiffness matrix and elemental mass matrix; α_i and β_i are, respectively, "elemental stiffness parameter" (ESP) and "elemental mass parameter" (EMP); and $[K^e]_i$ and $[M^e]_i$ are, respectively, the elemental stiffness matrix and elemental mass matrix divided by α_i and β_i. For example, for the Euler–Bernoulli beam model without considering the axial deformation, ESP is the elemental bending stifiness (EI) and EMP is the elemental mass per unit length (ρ). Similarly the changed stiffness matrix is given by

$$[\tilde{K}] = \sum_{i=1}^{m}[\tilde{K}]_i = \sum_{i=1}^{m}\tilde{\alpha}_i[K^e]_i \tag{10}$$

and

$$[\Delta K] = [\tilde{K}] - [K] = \sum_{i}^{m}([\tilde{K}]_i - [K]_i) = \sum_{i=1}^{m}(\tilde{\alpha}_i - \alpha_i)[K^e]_i = \sum_{i=1}^{m}\Delta\alpha_i[K^e]_i, \tag{11}$$

where $\tilde{\alpha}_i$ is the ESP in the changed state and $\Delta\alpha_i$ is the ESP reduction. Substituting Eq. (11) into Eq. (7), the equations can be written in the form of

$$[S]\{\Delta\alpha\} = \{\Delta\lambda\}, \tag{12}$$

where $\{\Delta\alpha\}$ and $(\Delta\lambda)$ are elemental stiffness reduction vector and eigenvalue change vector, respectively, and $[S]$ is the sensitivity matrix whose elements are

$$S_{ij} = \{\phi_i\}^{\mathrm{T}}[K^e]_j\{\phi_i\} \tag{13}$$

for $i = 1, 2, \ldots, n$ and $j = 1, 2, \ldots, m$, where n is the number of available frequencies in testing. When the initial FE model is known and the frequencies in the changed state are measured accurately, Eq. (12) can be uniquely solved and $\{\Delta\alpha\}$ is derived if the matrix $[S]$ is square. But in practice, the number of measured frequencies n is usually less than the unknown variables m. Therefore, this is an underdetermined problem in mathematics and has infinite solutions. Normally, the minimum norm solution is derived with the assumption that the norm of $\{\Delta\alpha\}$ is minimum, i.e., stiffness changes are minimized [5]. Therefore,

$$\{\Delta\alpha\} = [S]^{+}\{\Delta\lambda\}, \tag{14}$$

where $[]^{+}$ is Moore–Penrose generalized inverse which can be solved by singular value decomposition. Thereafter the ESP in the updated model, $\tilde{\alpha}_i$, is simply obtained by $\tilde{\alpha}_i = \alpha_i + \Delta\alpha_i$. A non-dimensional parameter, "stiffness reduction factor" (SRF) is defined as the ratio of $\Delta\alpha_i$ to α_i. It varies between -1 and 0. The negative values of SRF locate the damaged elements, and the values represent the damage severity.

3. Error analysis

The above algorithm is developed based on the assumption that both the FE model and the measured modal data are accurate. But in real applications, errors always exist which may lead to incorrect damage identification results. Therefore, it is very important to investigate the influence of the FE modelling error and measurement noise on the identification results. Modelling errors generally include discretization error, configuration error and mechanical parameter error. As discussed above, in this study, only the random errors associated with the structural material properties, in particular, with EI, are considered. Investigation from literatures finds that these random errors usually have normal distribution [14]. The errors that occur in the measured modal data may be divided into two classes: biased (systematic) error and random error. Biased error is caused by malfunction of equipment or/and environment sources. It might not have zero mean and have different types of distributions. Random error, on the other hand, has zero mean and is usually modelled as normally distributed. Detailed discussion can be seen in Bendat and Piersol [15]. In this paper, as discussed above, again only random error in the measured modal data are considered. Random noises in the measured vibration data are usually assumed having normal distributions in the analysis [9,11,16].

In the present study, the uncertainties of the FE model and the measurement data are also assumed as normally distributed random variables with zero means and given covariance. The quantities are equal to the true values plus the random noises as

$$\tilde{\lambda}_i = \tilde{\lambda}_i^0 + \tilde{\lambda}_i^0 X_{\lambda i} = \tilde{\lambda}_i^0 (1 + X_{\lambda i}), \tag{15}$$

$$\alpha_j = \alpha_j^0 + \alpha_j^0 X_{\alpha j} = \alpha_j^0 (1 + X_{\alpha j}), \tag{16}$$

$$\beta_j = \beta_j^0 + \beta_j^0 X_{\beta j} = \beta_j^0 (1 + X_{\beta j}) \tag{17}$$

for $i = 1, 2, \ldots, n$ and $j = 1, 2, \ldots, m$, where superscript "0" represents the corresponding true value, $X_{\lambda i}$, $X_{\alpha j}$, and $X_{\beta j}$ are the relative random noises in the measured eigenvalues, ESP and EMP,

respectively. For simplicity, $X_{\lambda i}$, $X_{\alpha j}$, $X_{\beta j}$ are written together as a vector X_i, $i = 1, 2, \ldots, n, n+1, \ldots, n+2m$. According to the above assumptions, $E(X_i) = 0$.

With perturbation technique [10], Eq. (12) is expanded as a second order Taylor series in terms of X_i,

$$[S] = [S]^0 + \sum_{i=1}^{n+2m} \frac{\partial [S]}{\partial X_i} X_i + \frac{1}{2} \sum_{i=1}^{n+2m} \sum_{j=1}^{n+2m} \frac{\partial^2 [S]}{\partial X_i \partial X_j} X_i X_j, \tag{18}$$

$$\{\Delta\alpha\} = \{\Delta\alpha\}^0 + \sum_{i=1}^{n+2m} \frac{\partial \{\Delta\alpha\}}{\partial X_i} X_i + \frac{1}{2} \sum_{i=1}^{n+2m} \sum_{j=1}^{n+2m} \frac{\partial^2 \{\Delta\alpha\}}{\partial X_i \partial X_j} X_i X_j, \tag{19}$$

$$\{\Delta\lambda\} = \{\Delta\lambda\}^0 + \sum_{i=1}^{n+2m} \frac{\partial \{\Delta\lambda\}}{\partial X_i} X_i + \frac{1}{2} \sum_{i=1}^{n+2m} \sum_{j=1}^{n+2m} \frac{\partial^2 \{\Delta\lambda\}}{\partial X_i \partial X_j} X_i X_j. \tag{20}$$

Substituting the above equations into Eq. (12) and comparing the terms of 1, X_i, and $X_i X_j$, then $\{\Delta\alpha\}^0$, $\partial\{\Delta\alpha\}/\partial X_i$, $\partial^2\{\Delta\alpha\}/\partial X_i \partial X_j$ $(i,j = 1, 2, \ldots, n+2m)$ can be solved one by one as

$$\{\Delta\alpha\}^0 = ([S]^0)^+ \{\Delta\lambda\}^0, \tag{21}$$

$$\frac{\partial \{\Delta\alpha\}}{\partial X_i} = ([S]^0)^+ \left(\frac{\partial \{\Delta\lambda\}}{\partial X_i} - \frac{\partial [S]}{\partial X_i} \{\Delta\alpha\}^0 \right), \tag{22}$$

$$\frac{\partial^2 \{\Delta\alpha\}}{\partial X_i \partial X_j} = ([S]^0)^+ \left(\frac{\partial^2 \{\Delta\lambda\}}{\partial X_i \partial X_j} - \frac{\partial^2 [S]}{\partial X_i \partial X_j} \{\Delta\alpha\}^0 - 2 \frac{\partial [S]}{\partial X_i} \frac{\partial \{\Delta\alpha\}}{\partial X_j} \right). \tag{23}$$

From Eq. (19) the mean values of $\{\Delta\alpha\}$ are, noting that $E(X_i) = 0$,

$$E(\{\Delta\alpha\}) = E(\{\Delta\alpha\}^0) + \frac{1}{2} \sum_{i=1}^{n+2m} \frac{\partial^2 \{\Delta\alpha\}}{\partial X_i^2} \mathrm{Cov}(X_i, X_i) \tag{24}$$

and the covariance matrix of $\{\Delta\alpha\}$ is

$$[\mathrm{Cov}(\Delta\alpha, \Delta\alpha)]_{m\times m} = \left[\frac{\partial \{\Delta\alpha\}}{\partial \{X\}} \right]_{m\times(n+2m)} [\mathrm{Cov}(X, X)]_{(n+2m)\times(n+2m)} \left[\frac{\partial \{\Delta\alpha\}}{\partial \{X\}} \right]^{\mathrm{T}}_{(n+2m)\times m}. \tag{25}$$

The subscripts in Eq. (25) are the dimensions of matrices. It is worth noting that the noise vector X includes three parts, namely λ_i, α_i and β_i whose covariance matrix will be given later.

From the above equations, in order to calculate the mean values and covariance matrix of $\{\Delta\alpha\}$, $\partial\{\Delta\lambda\}/\partial X_i$, $\partial[S]/\partial X_i$, $\partial^2\{\Delta\lambda\}/\partial X_i^2$ and $\partial^2[S]/\partial X_i^2$ must be derived and whose elements are given as

$$\frac{\partial \Delta\lambda_i}{\partial X_k} = \frac{\partial \tilde{\lambda}_i}{\partial X_k} - \frac{\partial \lambda_i}{\partial X_k}, \tag{26}$$

$$\frac{\partial S_{ij}}{\partial X_k} = \frac{\partial (\{\phi_i\}^{\mathrm{T}} [K^e]_j \{\phi_i\})}{\partial X_k} = 2\{\phi_i\}^{\mathrm{T}} [K^e]_j \frac{\partial \{\phi_i\}}{\partial X_k}, \tag{27}$$

$$\frac{\partial^2 \Delta\lambda_i}{\partial X_k^2} = \frac{\partial^2 \tilde{\lambda}_i}{\partial X_k^2} - \frac{\partial^2 \lambda_i}{\partial X_k^2}, \tag{28}$$

$$\frac{\partial^2 S_{ij}}{\partial X_k^2} = 2\{\phi_i\}^{\mathrm{T}}[K^e]_j \frac{\partial^2 \{\phi_i\}}{\partial X_k^2} + 2\frac{\partial^2 \{\phi_i\}^{\mathrm{T}}}{\partial X_k}[K^e]_j \frac{\partial \{\phi_i\}}{\partial X_k} \tag{29}$$

for $i = 1, 2, \ldots, n$, $j = 1, 2, \ldots, m$ and $k = 1, 2, \ldots, n+2m$. It is noted that $[K^e]_j$, λ_i and ϕ_i are independent of measurement noise, thus their derivatives to X_k, $k = 1, 2, \ldots, n$ are zero. Similarly, the derivatives of $\tilde{\lambda}_i$ to X_k, $k = n+1, n+2, \ldots, n+2m$, are zero. From Eq. (15), it is easy to find that

$$\frac{\partial \tilde{\lambda}_i}{\partial X_k} = \tilde{\lambda}_i^0 \quad \text{and} \quad \frac{\partial^2 \tilde{\lambda}_i}{\partial X_k^2} = 0, \quad k = 1, 2, \ldots, n. \tag{30}$$

The first and second partial derivative of the analytical eigenvalues and eigenvectors with respect to the ESP and EMP can be computed according to Fox and Kapoor [17]. Thereby, Eqs. (26)–(29) are obtained.

Substituting Eqs. (26)–(29) into Eqs. (22) and (23), the mean values and covariance matrix of $\{\Delta\alpha\}$ are estimated according to Eqs. (24) and (25). Therefore, the statistics of ESP of the updated model can be obtained as

$$E(\tilde{\alpha}_i) = E(\alpha_i) + E(\Delta\alpha_i) = \alpha_i^0 + E(\Delta\alpha_i), \tag{31}$$

$$\begin{aligned} \mathrm{Cov}(\tilde{\alpha}_i, \tilde{\alpha}_j) &= \mathrm{Cov}(\alpha_i + \Delta\alpha_i, \alpha_j + \Delta\alpha_j) \\ &= \mathrm{Cov}(\alpha_i, \alpha_j) + \mathrm{Cov}(\alpha_i, \Delta\alpha_j) + \mathrm{Cov}(\Delta\alpha_i, \alpha_j) + \mathrm{Cov}(\Delta\alpha_i, \Delta\alpha_j), \end{aligned} \tag{32}$$

$\mathrm{Cov}(\Delta\alpha_i, \Delta\alpha_j)$ is given in Eq. (25), and from Eqs. (16) and (19), it has

$$\mathrm{Cov}(\alpha_i, \alpha_j) = \alpha_i^0 \alpha_j^0 \,\mathrm{Cov}(X_{\alpha i}, X_{\alpha j}), \tag{33}$$

$$\begin{aligned} \mathrm{Cov}(\alpha_i, \Delta\alpha_j) &= E\lfloor (\alpha_i - \alpha_i^0)(\Delta\alpha_j - \Delta\alpha_j^0) \rfloor \\ &= E\left[(\alpha_i^0 X_{\alpha i}) \left(\sum_{k=1}^{n+2m} \frac{\partial \Delta\alpha_j}{\partial X_k} X_k \right) \right] \\ &= \alpha_i^0 \sum_{k=1}^{n+2m} \frac{\partial \Delta\alpha_j}{\partial X_k} E(X_{\alpha i} X_k) \\ &= \alpha_i^0 \sum_{k=1}^{n+2m} \frac{\partial \Delta\alpha_j}{\partial X_k} \mathrm{Cov}(X_{\alpha i}, X_k) \end{aligned} \tag{34}$$

and similarly

$$\mathrm{Cov}(\Delta\alpha_i, \alpha_j) = \mathrm{Cov}(\alpha_j, \Delta\alpha_i) = \alpha_j^0 \sum_{k=1}^{n+2m} \frac{\partial \Delta\alpha_i}{\partial X_k} \mathrm{Cov}(X_{\alpha j}, X_k). \tag{35}$$

Then from Eq. (32), the standard deviation of $\tilde{\alpha}_i$, $\sigma(\tilde{\alpha}_i)$, can be derived as the square root of the corresponding diagonal element of the covariance matrix. The statistics of $\{\tilde{\alpha}\}$ derived above with perturbation method will be verified by Monte Carlo simulation.

The closed-form solution of the statistical distribution of $\{\tilde{\alpha}\}$ is very difficult to derive. This is because $\{\Delta\alpha\}$ is non-linearly related to the ESP, EMP and eigenvalues as defined in Eq. (14). Since Monte Carlo simulations give statistical samples of $\{\tilde{\alpha}\}$, those samples can be used to derive their distributions. As will be shown later in a numerical example, the statistical distributions of ESPs in the updated model also have normal type distribution. The above statistical model updating procedure can be applied to the two-stage model updating presented in this paper to derive the statistical distributions of the stiffness parameters of UM and DM, respectively.

4. Probability of damage existence (PDE)

The PDE can be estimated from the statistical distributions of the stiffness parameters of UM and DM. The basic idea is to compute the probability of an ESP at a confidence level. For example, for an element i, its stiffness parameter in the intact state α_i is assumed as a normally distributed variable with a mean $E(\alpha_i)$ and a standard deviation $\sigma(\alpha_i)$, then its probability density function (PDF) is as illustrated in Fig. 2. The interval of the healthy stiffness parameter, $\Omega(\alpha_i, \mu)$ is defined so that the probability of α_i contained within the interval is μ, i.e.,

$$\text{prob}(x_\alpha \in \Omega(\alpha_i, \mu)) = \text{prob}(L_\Omega \leqslant x_\alpha < \infty) = \mu, \tag{36}$$

where L_Ω is the lower bound of the interval $\Omega(\alpha_i, \mu)$, which can be easily obtained for normal distribution, $\Omega(\alpha_i, \mu)$ depends on the required confidence level. In statistical analysis of this study, we set μ to 95%, thus $L_\Omega = E(\alpha_i) - 1.645\sigma(\alpha_i)$, indicating there is a probability of 95% that the healthy stiffness parameter falls in the range of $[E(\alpha_i) - 1.645\sigma(\alpha_i), \infty)$.

Similarly the stiffness parameter damaged state $\tilde{\alpha}_i$ is also assumed as a normally distributed variable with a mean $E(\tilde{\alpha}_i)$ and a standard deviation $\sigma(\tilde{\alpha}_i)$ the corresponding PDF of $\tilde{\alpha}_i$ is also plotted in Fig. 2. The PDE is defined as that of $\tilde{\alpha}_i$ not within the 95% confidence healthy interval $\Omega(\alpha_i, 0.95)$. Thus the PDE of an element i is

$$\begin{aligned} p_d^i &= 1 - \text{prob}(x_{\tilde{\alpha}} \in \Omega(\alpha_i, 0.95)) = 1 - \text{prob}(L_\Omega \leqslant x_{\tilde{\alpha}} < \infty) \\ &= \text{prob}(-\infty < x_{\tilde{\alpha}} \leqslant L_\Omega). \end{aligned} \tag{37}$$

Fig. 2 shows the healthy area and PDE area as denoted by P_d^i.

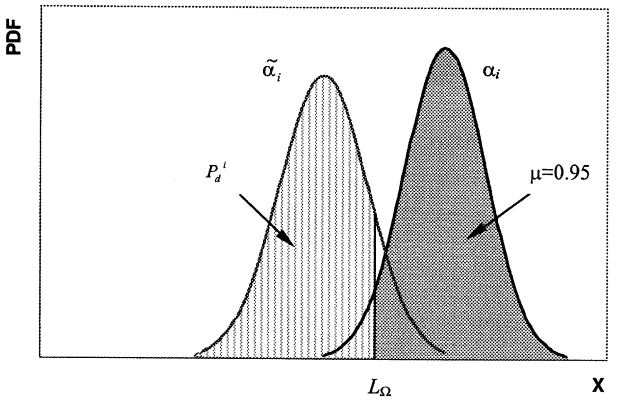

Fig. 2. Probability density functions of $\tilde{\alpha}_i$, α_i, and PDE, p_d^i.

PDE is a value between 0 and 1. It is apparent that if the PDE of an element is close to 1 then most likely the element is damaged; and on the other hand, if the PDE is close to 0, the damage of the element is very unlikely. However, it is difficult to give a threshold of PDE for damage identification, because it depends on the confidence level of FE modelling and the measured data.

The steps of probabilistic damage identification are given in the following:

1. establish the random FE model of initial structure (IM) by including the statistical variations of ESP and EMP;
2. perform statistical model updating to determine the distributions of ESP in the undamaged structure (UM), if measurement of eigenvalues is available; otherwise, skip this step and distributions of ESP in UM is directly determined in Step 1;
3. add random noises into the measured eigenvalues of the damaged structure, perform second-stage statistical model updating to determine the statistical properties of DM and then derive the distributions of ESP in DM;
4. Estimate the PDE for each element of the structure based on statistical ESP derived for UM and DM.

5. Numerical example

To illustrate the proposed statistical damage identification method, a steel cantilever beam is first utilized to numerically demonstrate the procedure.

Fig. 3 is the FE model of the intact beam with 9 Euler–Bemoulli elements (i.e., $m = 9$). The actual Young's modulus in the intact state is $2.0 \times 10^{11}\,\mathrm{N/m^2}$, the size of the cross-section is $50.75 \times 6.0\,\mathrm{mm^2}$ and the mass density is $7.67 \times 10^3\,\mathrm{kg/m^3}$. Assuming element 5 is damaged with the bending stiffness degraded by 20%. In practice, the actual structural stiffness parameters have more uncertainties than the mass parameters, thus in the initial analytical model the ESPs are assumed as 1.1 times the actual ones and the EMPs are accurate. Thus, the ESPs of the initial analytical model (IM), the actual undamaged model (UM) and the damage model (DM) are, $\alpha_{1-9}^{IM} = 182.7 \times 1.1 = 200.97\,\mathrm{N\,m^2}$, $\alpha_{1-9}^{UM} = \alpha_{1-4,6-9}^{DM} = 182.7\,\mathrm{N\,m^2}$ and $\alpha_5^{DM} = 182.7 \times 0.8 = 146.16\,\mathrm{N\,m^2}$, respectively. Assuming the first 6 frequencies are measured (i.e., $n = 6$), which for the three models are derived with eigenvalue analysis and listed in Table 1.

5.1. Statistical model updating in the first stage

As stated before, the initial analytical FE model (IM) and the measured frequencies are inevitably smeared with errors. To investigate their effects, in the first updating stage, normally

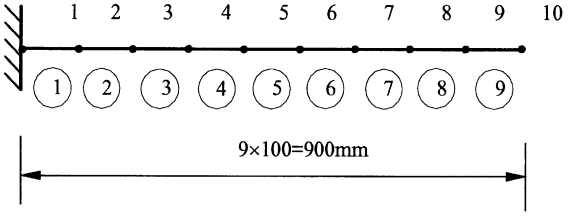

Fig. 3. FE model of the cantilever beam.

distributed random noises with zero means are added to the IM and the measured frequencies in the undamaged state to derive a tuned FE model for UM. Assuming the random noises are independent of each other, the covariance matrix of noises is a 24×24 diagonal matrix (6 for measured frequencies, 9 for ESP and 9 for EMP). Without loss of generality, the noise level is set to be 1%, which means the standard deviation of the random noise is equal to 1% of the corresponding true quantity (mean value). Therefore,

$$\mathrm{Cov}(X_i, X_j) = \begin{cases} 0 & \text{for } i \neq j, \\ (1\%)^2 & \text{for } i = j \end{cases} \tag{38}$$

for $i, j = 1, 2, \ldots, 24$.

Using the perturbation method, the mean values and standard deviations of ESP in the undamaged state (UM) are computed and illustrated in Fig. 4. To verify the results, Monte Carlo technique is also applied and the results after 10,000 simulations are also shown in the figure. It shows that the two algorithms yield very similar results, indicating the perturbation method based on the second order Taylor series expansion is reliable. For convenience, the coefficients of variation, i.e., the ratios of standard deviations to the corresponding mean values are presented in the figure rather than the standard deviations themselves.

The figure also illustrates that the coefficients of variation of ESP are about 3–15% when the noise level is 1%, this implies that the uncertainties are enlarged after the model updating. To investigate which type of noise has more significant influence on the updated ESP, the sensitivities of the updated ESP with respect to the measurement noise, ESP error and EMP error are

Table 1
Natural frequencies of the IM, UM and DM (Hz)

Model	Mode					
	1	2	3	4	5	6
IM	6.41	40.14	112.44	220.56	365.44	548.18
UM	6.11	38.27	107.20	210.30	348.44	522.67
DM	6.07	37.27	107.02	205.59	346.67	513.30

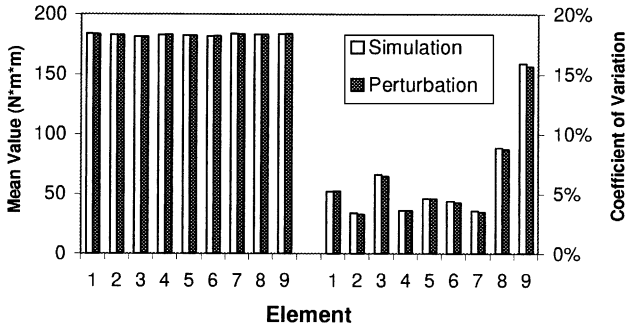

Fig. 4. Mean values and coefficients of variation of ESP in the undamaged state.

investigated. First only the measured eigenvalues are smeared with 1% random noise and the analytical FE model is accurate without statistical variations. Then the above model updating procedure is applied to derive the ESP in the undamaged state. The root mean square of the coefficients of variation of ESP is derived. This procedure is repeated separately by considering ESP error only and EMP error only with 1% variation. The root mean square values of coefficients of variation for the three types of uncertainties are, respectively, 7.73%, 0.63% and 0.90%. They indicate that the updated ESP is much more sensitive to the measurement noise than the FE modelling errors.

5.2. Distribution test

As discussed above, the closed-form solution of probabilistic distribution of the updated ESP is difficult to derive. But the Monte Carlo simulation results indicate that it has normal type characteristics. This observation needs to be verified by goodness-of-fit test technique. Commonly used goodness-of-fit test methods, such as chi-squared goodness-of-fit test and Kolmogorov–Smirnov (K–S) goodness-of-fit test [18,19], are applied in this paper to verify the distributions of ESPs of the updated model.

The samples of updated ESPs can be obtained from the Monte Carlo simulation results. For example, after 100 times simulation, there is a sample with a size of 100 for each updated ESP whose mean and standard deviation can be estimated from the 100 sample points. Then the sample of each element is tested at a confidence level of 95%. Fig. 5 shows the chi-squared goodness-of-fit test and K–S goodness-of-fit test for element 2. Fig. 5(a) is the observed and theoretical frequencies of the non-overlapping groups, and Fig. 5(b) gives the cumulative distribution function (CDF) calculated from the sample points as compared with the theoretical one. Based on the goodness-of-fit test approach, normal distribution hypothesis of the stiffness parameters for all the elements is accepted with a confidence level of 95%.

5.3. Statistical model updating in the second stage

From the statistical model in the undamaged state UM, the damaged model DM is also derived by statistical model updating with the measured frequencies in the damaged state. The measured frequencies are also smeared with normally distributed random noises. Again both the perturbation method and Monte Carlo technique (after 10,000 simulations) are used, the mean values and coefficients of variation of ESPs of DM are computed. The results with two algorithms are again very close.

Similarly, the probabilistic distributions of the ESPs in the updated damaged model DM are assumed as Gaussian, and the hypothesis is tested by chi-squared goodness-of-fit test and K–S goodness-of-fit test. The results, not shown here, also indicate that all the ESPs of DM are normally distributed at a 95% confidence level.

5.4. Probability of damage existence (PDE)

After the distributions of the ESPs in the undamaged and damaged states are both estimated, the PDE can be obtained for every element from Eq. (37) and listed in the third row of Table 2. It

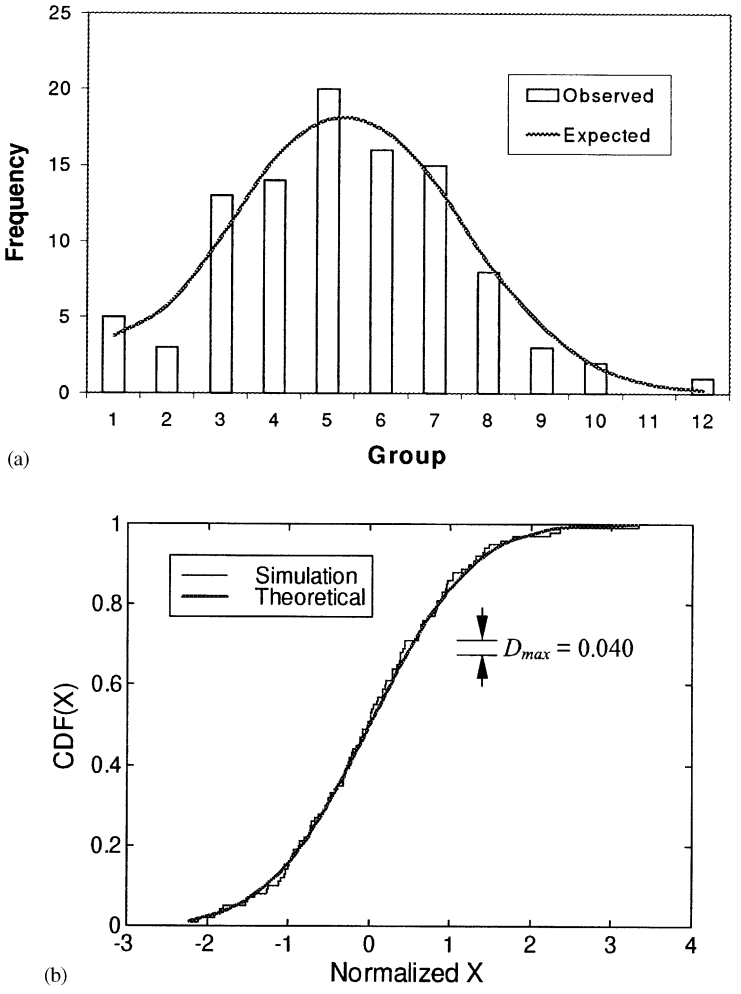

Fig. 5. Hypothesis test for element 2 in the undamaged state: (a) chi-square goodness-of-fit test and (b) K–S goodness-of-fit test.

clearly indicates that element 5 is most likely damaged with very high probability. The PDE values of other elements are less than 10%, and thus these elements can be considered as undamaged.

5.5. *Mode effect*

In the above calculation, it is assumed that the first 6 frequencies are measured. In a real structure, the number of measurable frequencies is usually about 30. It is believed that the more measured information, here modal frequencies, is available, the more accurate damage identification results will be, despite of more noises will be introduced with the more measurement data. To investigate this, the above analysis is performed again but by assuming that only first 3, 4 and 5 modal frequencies are available in each analysis. The PDEs are obtained and compared in Table 2. It shows that with less number of modal frequencies, the damaged element 5 still can be

Table 2
Probability of damage existence when different modes used, $SRF(5) = -20\%$

Modes	Element (%)								
	1	2	3	4	**5**	6	7	8	9
1–6	7.4	9.2	1.6	6.9	**99.8**	2.3	7.0	3.2	1.8
1–5	29.2	0.2	0.5	0.2	**99.5**	3.2	3.2	8.4	1.2
1–4	9.3	5.2	0.0	6.2	**99.9**	16.7	0.3	29.9	7.4
1–3	67.2	0.0	0.0	66.8	**96.8**	91.3	0.1	0.0	1.6

confidently identified, but more undamaged elements might be falsely detected as damaged. For example, if only the first 3 frequencies are available, the undamaged elements 1, 4 and 6 are also associated with high PDE values, implying false identification. These observations indicate that the confidence of damage identification reduces when less modal frequencies are measured. In this example, at least the first 4 modal frequencies are necessary in order to give a successful identification analysis. But it is difficult to give a general criterion on how many modes are enough for successful damage identification analysis as it depends on structural types, number of damages and their locations. It deserves further study.

5.6. Parameter study

From the results, it can be seen that the true damaged element can be identified by the developed method even the statistical FE modelling error and measurement noise are included in the consideration. However, the accuracy and confidence of the identification results depend on the relative levels of statistical uncertainties and damage severity. If the uncertainties in FE model and measured modal data are significant than the effect of structural damage on its vibration properties, it will be unlikely to have a reliable damage identification calculation. To investigate the sensitivity of damage levels, numerical analyses are performed by assuming different structural damage levels while the uncertainty level is kept unchanged with 1% standard deviation.

Assuming that element 5 is damaged with SRF equals to -5%, -10%, -15%, -20%, -25%, -30%, and -40%, respectively, the PDEs of every element in different damage levels are computed and listed in Table 3.

For all the cases considered, the PDE of element 5 is higher than those of other elements, implying that the element has higher PDE. It is found that when the damage is insignificant, for example in the case of SRF equals to -5%, the PDE of element 5 is not high, which means that the damage cannot be detected confidently. This is because the frequency changes are not apparent in the case and the noises of measurement and modelling errors may make the small changes intangible. With the increase of the damage severity, the calculated PDE of element 5 increases sharply and monotonously but others do not. Therefore, the damage identifiability is improved. The calculated PDEs of other elements change with respect to the damage level of element 5. This is because of the non-linear effect caused by severe damage in one of the structural elements, as will be further discussed later. Particularly, when the damage is severe ($SRF = -30\%$), the PDE of element 1 increases to about 18%, and it is about 37% when $SRF = -40\%$. This might lead to false identification.

Table 3
Probability of damage existence in different damage levels

Damage level (%)	Element (%)								
	1	2	3	4	**5**	6	7	8	9
−5	4.4	11.0	4.1	10.6	**22.9**	3.0	6.3	2.6	2.4
−10	4.4	11.3	2.6	9.6	**65.9**	2.6	8.0	2.4	1.9
−15	4.7	9.5	2.3	8.4	**93.7**	2.5	7.4	1.6	1.4
−20	7.4	9.2	1.6	6.9	**99.8**	2.3	7.0	3.2	1.8
−25	8.5	7.6	0.9	6.3	**100.0**	3.3	6.5	3.8	1.8
−30	17.9	6.6	0.5	4.4	**100.0**	3.3	7.8	3.8	1.4
−40	37.1	3.4	0.2	2.0	**100.0**	2.0	5.5	7.4	0.4

Table 4
Probability of damage existence, $SRF(5) = -40\%$

Element	1	2	3	4	**5**	6	7	8	9
Without iterations (%)	37.1	3.4	0.2	2.0	**100.0**	2.0	5.5	7.4	0.4
With 20 iterations (%)	15.1	4.2	3.0	4.6	**100.0**	4.7	8.1	8.4	5.6

To reduce the non-linear effect, Eq. (14) can be solved iteratively. To demonstrate that, the case with $SRF = -40\%$ is used as an example, 20 iterations are performed with the same statistical damage identification procedure. Table 4 compares the results of PDEs with and without iterations. It shows that the PDE of element 1 decreases to 15% after iterations are applied, indicating a substantial improvement on the accuracy of damage identification results.

5.7. *Multiple damages*

To further illustrate the effectiveness of the proposed damage identification algorithm, the case of multiple damages is studied. For the same cantilever beam, assume that elements 1 and 5 are damaged with SRFs of −20%. Noise levels are the same as above. The PDEs of all the elements are similarly computed and listed in Table 5. It can be seen that the PDEs of the two damaged elements are the highest among all elements, again implying that the elements have higher probabilities of damage occurrence. But element 2 also has a high PDE, due to the non-linear effect associated with severe damage of structural elements, as discussed in the previous example. Again, 20 iterations are performed and the results are also listed in Table 5. It shows that the PDE of element 1 increases and PDE of element 2 decreases to 12% after iterations.

6. Experimental example

A steel cantilever plate tested by Friswell et al. [13] is applied here to further illustrate the proposed algorithm. Fig. 6 shows the FE mesh and the saw cuts. The analytical natural

frequencies are shown in Table 6 along with the measured frequencies before and after the artificial damage.

Because the plate is symmetric, only the stiffness parameters of elements 1–8 are adjusted during model updating [5]. With the present probabilistic damage identification procedure, PDEs of elements 1–8 are estimated and listed in Table 7. It shows that the PDE of element 2 is much higher than other elements, implying that the element has higher PDE. Therefore, the true damage is detected correctly.

7. Conclusions

A statistical damage identification algorithm based on perturbation method has been presented in this paper with two-stage model updating. The statistics of the stiffness parameters of the undamaged and damaged structure are, respectively, derived by considering both the statistical variations of the FE modelling errors and measurement noises in the first- and second-stage updating. With the assumption that the statistical variations of the structural parameters and the measured vibration data have normal distributions, the statistical distributions of the stiffness parameters of the updated FE model for the undamaged and damaged structure are proved also normal. Using the distributions of the undamaged and damaged stiffness parameters, the PDE for each structural element is estimated.

Table 5
Probability of damage existence, $SRF(1, 5) = -20\%$

Element	**1**	2	3	4	**5**	6	7	8	9
Without iterations (%)	**91.2**	41.3	3.2	12.4	**100.0**	4.3	6.7	1.5	1.2
With 20 iterations (%)	**99.2**	11.8	4.9	8.9	**99.5**	3.6	8.4	8.6	5.4

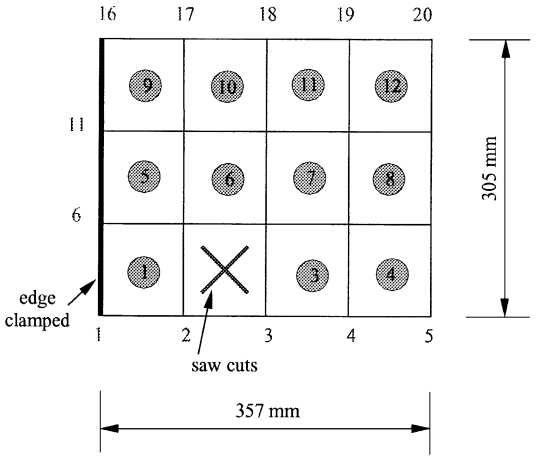

Fig. 6. FE model of the cantilever plate (shaded number is element number).

Table 6
Analytical and measured frequencies (Hz)

Mode	Analytical	Measurement	
		Undamaged	Damaged
(1)	(2)	(3)	(4)
1	20.2	20.0	19.6
2	55.9	56.7	55.7
3	126.5	124.6	120.8
4	195.5	198.1	193.4
5	202.8	212.6	209.6
6	358.9	353.9	343.0
7	361.2	380.8	377.8
8	415.1	427.5	415.5
9	509.5	530.1	521.1
10	595.1	639.9	622.4
11	636.2	690.7	666.2
12	704.0	N/A	N/A
13	721.1	774.5	749.3

Table 7
Probability of damage existence of the plate

Element	1	**2**	3	4	5	6	7	8
PDE (%)	4.0	**65.0**	18.0	12.0	11.0	17.0	6.0	3.0

A cantilever beam with single damage and multiple damages and a laboratory tested steel cantilever plate have been used to illustrate the procedure. Numerical results demonstrated that the true damaged elements can be identified with higher probabilities of damage existence than the undamaged ones.

References

[1] S.W. Doebling, C.R. Farrar, M.B. Prime, D.W. Shevitz, Damage identification and health monitoring of structural and mechanical systems from changes in their vibration characteristics: a literature review, Los Alamos National Laboratory Report LA-13070-MS, 1996.
[2] P. Cawley, R.D. Adams, The location of defects in structures from measurements of natural frequencies, Journal of Strain Analysis 14 (2) (1979) 47–49.
[3] U. Meneghetti, A. Maggiore, Crack detection by sensitivity analysis, Proceedings of the 12th International Modal Analysis Conference, Honolulu, HI, 1994, pp. 1292–1298.
[4] J.M.M. Silva, A.J.M.A. Gomes, Crack identification of simple structural elements through the use of natural frequency variations: the inverse problem, Proceedings of the 12th International Modal Analysis Conference, Honolulu, HI, 1994, pp. 1728–1735.
[5] S. Hassiotis, G.D. Jeong, Identification of stiffness reduction using natural frequencies, Journal of Engineering Mechanics, American Society of Civil Engineers 121 (10) (1995) 1106–1113.

[6] A. Morassi, N. Rovere, Localizing a notch in a steel frame from frequency measurements, Journal of Engineering Mechanics, American Society of Civil Engineers 123 (5) (1997) 422–432.
[7] J.M.W. Brownjohn, P.Q. Xia, H. Hao, Y. Xia, Civil structure condition assessment by FE model updating: methodology and case studies, Finite Elements in Analysis and Design 37 (10) (2000) 761–775.
[8] M.I. Friswell, J.E.T. Penny, S.D. Garvey, Parameter subset selection in damage location, Inverse Problems in Engineering 5 (3) (1997) 115–189.
[9] J.D. Collins, G.C. Hart, T.K. Hasselman, B. Kennedt, System identification of structures, American Institute of Aeronautics and Astronautics Journal 12 (2) (1974) 185–190.
[10] P.L. Liu, Identification and damage detection of trusses using modal data, Journal of Structural Engineering, American Society of Civil Engineers 121 (4) (1995) 599–608.
[11] L. Papadopoulos, E. Garcia, Structural damage identification: a probabilistic approach, American Institute of Aeronautics and Astronautics Journal 36 (11) (1998) 2137–2145.
[12] N. Bicanic, H.P. Chen, Damage identification in framed structures using natural frequencies, International Journal for Numerical Methods in Engineering 40 (1997) 4451–4468.
[13] M.I. Friswell, J.E.T. Penny, D.E.L. Wilson, Using vibration data and statistical measures to locate damage in structures, Modal Analysis: The International Journal of Analytical and Experimental Modal Analysis 9 (4) (1994) 239–254.
[14] H.Y. Low, H. Hao, Reliability analysis of reinforced concrete slabs under explosive loading, Structural Safety 23 (2001) 157–178.
[15] J.S. Bendat, A.G. Piersol, Engineering Applications of Correlation and Spectral Analysis, Wiley, New York, 1993.
[16] Y. Xia, H. Hao, Measurement selection for vibration-based structural damage identification, Journal of Sound and Vibration 236 (1) (2000) 89–104.
[17] R.L. Fox, M.P. Kapoor, Rate of change of eigenvalues and eigenvectors, American Institute of Aeronautics and Astronautics Journal 6 (12) (1968) 2426–2429.
[18] N.T. Kottegoda, R. Rosso, Statistics, Probability, and Reliability for Civil and Environmental Engineers, McGraw-Hill, New York, 1997.
[19] W.H. Press, S.A. Teukolsky, W.T. Vetterling, B.P. Flannery, Numerical Recipes in FORTRAN: The Art of Scientific Computing, Cambridge University Press, Cambridge, 1992.